Mapping the geoid for Iberia and the Macaronesian Islands using multisensor gravity data and the GRACE geopotential model

J. Catalão, M.J. Sevilla

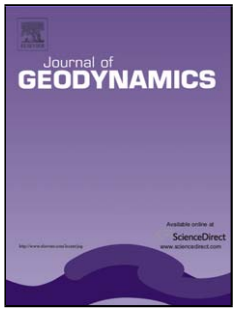

Title: Mapping the geoid for Iberia and the Macaronesian Islands using multisensor gravity data and the GRACE geopotential model

Authors: J. Catalão, M.J. Sevilla

PII: S0264-3707(09)00037-4
DOI: doi:10.1016/j.jog.2009.03.001
Reference: GEOD 880

To appear in: *Journal of Geodynamics*

Received date: 31-7-2008
Revised date: 23-3-2009
Accepted date: 23-3-2009

Please cite this article as: Catalão, J., Sevilla, M.J., Mapping the geoid for Iberia and the Macaronesian Islands using multisensor gravity data and the GRACE geopotential model, *Journal of Geodynamics* (2008), doi:10.1016/j.jog.2009.03.001

Mapping the geoid for Iberia and the Macaronesian Islands using multi-sensor gravity data and the GRACE geopotential model

J. Catalão[1], M. J. Sevilla[2]

[1] University of Lisbon, Faculty of Sciences, IDL, LATTEX, Lisbon, jcfernandes@fc.ul.pt

[2] Instituto de Astronomía y Geodesia, UCM-CSIC, Madrid, sevilla@mat.ucm.es

Abstract

A new gravimetric geoid model (ICAGM07) has been determined for the North-East Atlantic Ocean, Iberia, and the Macaronesian Islands using multi-sensor gravity data and a GRACE derived Earth geopotential model. A high resolution gravity model, determined using least squares optimal interpolation of marine, land, and satellite derived gravity anomalies, was used to resolve the medium and short wavelengths of the geoid. Long wavelengths of the geoid were provided by the GRACE derived Earth geopotential model. The topographic effects were computed in the spectral domain using a high resolution (100 m) digital terrain model derived from SRTM mission data and cartographic charts. The remove-restore technique was used to compute the geoid model on a 1.5 arc minute grid, and the residual geoid height was computed using spherical FFT and a modified Stokes' kernel. The effects of different Earth tide models on the geoid were computed and analyzed. Comparison over the sea with an oceanographic geoid determined from CLS01 MSSH and Rio05 MDT yield a relative accuracy of 8 cm, with larger differences close to the shoreline. Over land, comparisons with 1646 GPS/levelling marks indicate an overall precision of 8-10 cm and relative vertical datum offsets of up to 2 m. This new geoid model represents a significant improvement over existing geoid models, with a homogeneous relative accuracy of 8-10 cm over both marine and land areas, and exposes the inaccuracies of local vertical datums as references for studies of vertical deformation.

Keywords: geoid, gravity, height unification, North Atlantic, Iberia

1. Introduction

The Iberia-Canary-Azores (ICA) gravity and geoid model is a project being undertaken by Iberian countries and is aimed at determining a high precision geoid model for Iberia, the Macaronesian Islands (Azores, Canary, and Madeira), and the North-East Atlantic. The main purpose of constructing this geoid surface is to enable connections to be made between the various different vertical reference systems in Iberia, the Azores, and Canary Islands, and also to establish the geoid as the reference surface for real time kinematics positioning within this geographic area. Further, this geoid model should be able to be used to recover dynamic sea-surface topography from satellite altimetry and thereby to derive oceanic circulation.

The ICA is a vast area extending from the mid-Atlantic ridge to the Balearic Islands in the Mediterranean Sea and from the Pyrenees to the Canary archipelago (Fig.1). It is a heterogeneous area, of which more than 70% is covered by sea, and includes the continental areas of Iberia and North Africa and three archipelagos with a total of 20 islands. The ICA is also a very dynamic area characterised by ongoing tectonic and volcanic activity, high gravity amplitudes and gradients, and a geoid gradient of about 10 m/degree on the Africa-Eurasian Plate boundary segment of south Portugal-Gibraltar Strait (Miranda et al. 1998).

The need for accurate geoid models has been driven by GPS users for ellipsoidal to orthometric height conversion aimed at the replacement of time-consuming levelling procedures. The geoid issue has attracted the interest of various national mapping agencies and of the geo-information community, and specific projects related to geoid computation have been implemented. Examples include: the densification of gravity measurements using land surveys or airborne surveys in remote areas

(Forsberg et al. 2000; Kern et al. 2003; Hwang et al. 2007; Scheinert et. al 2007); the investment in dedicated satellite gravity missions CHAMP (Reigber et al. 2002) and GRACE (Tapley et al. 2005), and in global high-resolution DTMs (Digital Terrain Models) derived from the SRTM (Shuttle Radar Topography Mission) (Bamler 1999); and the development of new methods and techniques for geoid computation (Gitlein et al. 2004; Schmidt and Kusche 2005; Serpas and Jekeli 2005; Sjöberg 2005; Klees et al. 2007; Prutkin and Klees 2007).

As a result, several regional geoid models have been determined for various land masses including Australia (Featherstone et al. 2001), Canada (Fotopoulos et al. 2000), Europe (Denker et al. 2005), Iran (Kiamehr 2006), Japan (Kuroishi et al. 2002), Gibraltar Strait (Sevilla 1997), and USA (Smith and Milbert 1999). Also, some geoid models, including the Artic geoid (Forsberg and Skourup 2005; Knudsen et al. 2006) and the Atlantic geoid (Fernandes et al. 2000; Vergos and Sideris 2003; Forsberg et al. 2004), have been determined for marine areas and have been more focused on oceanographic issues.

The explicit separation between marine and land geoid models is based on practical rather than conceptual (or theoretical) considerations, being motivated mainly by the use/application of the model. It is not usual to have geoid models covering land and marine areas with high (sub-decimetre) and homogeneous accuracy over both domains (Tziavos et al. 2005; Vergos et al. 2005). The main reason for this is that there are specific difficulties associated with the land/sea transition, related variously to the lack of offshore gravity and bathymetry data, to satellite altimetry data degradation (Rodriguez-Velasco et al. 2002; Fernandes et al. 2006), or to discontinuities in topographic/bathymetric databases.

Therefore, the main purpose of this paper is to address the problems associated with the determination of a geoid model for land and marine areas, with high and homogeneous accuracy for both domains, with particular respect to the ICA area. A geoid model was first computed for the ICA area by Catalão and Sevilla (1998) with sparse marine gravity data and rough DTMs using the remove-restore

technique, and the geoid was estimated by least squares collocation. Other gravimetric geoid solutions have been attempted by Fernandes et al. (2000) for the Azores area and Arabelos et al. (1999) for the Iberian coast, both using FFT techniques. Several other studies have considered, respectively, the effect of bathymetry on the estimation of the geoid (Catalão and Sevilla 1999), satellite altimetry data processing (Fernandes et al. 2006), the adjustment and validation of marine gravity data (Catalão and Sevilla 2004), the merging of multi-source gravity data (Catalão 2006), and the effect of mass density on the estimation of the geoid (Catalão and Bos 2008).

In this study, a new gravimetric solution for the ICA area is computed by means of spherical FFT with state-of-the-art data validation and treatment methods, using updated heterogeneous data (measured marine and land gravity, and satellite derived anomalies). Recently released geopotential models based on geopotential missions (CHAMP and GRACE) and a global DTM from the SRTM mission are incorporated into the ICA geoid model. The Earth tide model is discussed and its impact on the comparisons evaluated. The resulting geoid surface is compared over sea with the CLS01 mean sea surface and the Rio05 mean dynamic topography (MDT), and over land with 1646 GPS/levelling points from 14 different vertical datums.

2. Data compilation

2.1 Land and marine gravity data

A concerted effort was made to compile all gravity observations made in the geographic area of interest. For that purpose, a gravity database was set up using a GIS (Geographic Information System). The database included absolute and relative (both land and marine) gravity observations collected from a large variety of data sources (including from public institutions, private organisations, and universities) and from different measuring instruments. Within the GIS the visual validation was simplified by using simple queries to the database using native SQL language.

Land data were supplied primarily by IGP (Instituto Geográfico Português), IGN (Instituto Geográfico Nacional, Spain), and IAG (Instituto de Astronomia y Geodesia, Spain). In addition, data were available from six absolute gravity stations (Flores, Faial, S. Miguel, Mertola, Gaia, and Madrid). Details concerning data acquisition and validation for the Iberian Peninsula can be found in Kol and Vasconcelos (2000) and in Sevilla et al. (1997), and for the Azores archipelago can be found in Catalão and Bos (2008). The observation errors for land data were estimated to be 0.5 mGal for gravity and better than 10 cm for the height of the station. The gravity surveys have generally been tied to both the first-order gravity network and the levelling network.

Marine gravity data were supplied by the NGDC (National Geophysical Data Centre, USA, GEODAS data, Version 4.1.18), and cover an area with the following limits: $20°<\varphi<50°, 40°W<\lambda<10°W$. Most of the data were acquired from institutions in the USA, in the United Kingdom, and in France during the period from 1970 to 2005. This data bank was improved with a gravimetric campaign held in 1997 under the scope of the PDIC/C/Mar project (Fernandes et al. 1998) and the AGMASCO project (Timmen et al. 2002). The complete data set used in this study, obtained from a simple merge of data files, was cleaned from repeated missions recorded in different data banks, and resulted in a data set containing 856141 data points and 824 tracks.

Track bias was determined through a global weighted adjustment of the external COE (Cross Over Error) (Catalão and Sevilla 2004). After the adjustment, the standard deviation of the COEs reduces to 3.8 mGal, from an initial rms of 12.3 mGal, with a minimum and maximum reduced to -29 and 47 mGal, respectively. The adjustment solution (bias) was applied to each track and the associated individual (i.e., for each track) estimated standard deviation was assigned to each observation belonging to a track. The resulting file contained 533,718 gravity anomaly observations each with an associated standard deviation that does not reflect the observation's estimated precision but the overall quality of the track to which it belongs.

The final database contained 101,264 gravity anomalies over land and 533,718 ship-track gravity anomalies over the Atlantic and Mediterranean seas. A new set of ship-track observations offshore from the Canary Islands was included, increasing the spatial density of gravity data for this area. All gravity data were then referred to IGSN71, and the GSR80 system was used for normal gravity. The geographical coordinates were transformed to the GRS80 ellipsoid. The distribution of gravity data for the area of interest is presented in Fig. 1.

2.2 Satellite altimeter derived gravity grid

There are several public domain altimeter derived gravity anomaly data sets with global coverage. These models, in grid format, were computed either directly from sea surface heights (KMS02; Andersen et al. 1999), or through deflections of the vertical (Sandwell and Smith 1997). KMS02 is one of a series of satellite derived gravity anomalies data sets supplied by Kort-og MatrikelStryrelsen and can be freely downloaded from ftp://ftp.spacecenter.dk/pub/GRAVITY/pub/GRAVITY.

Numerous comparisons between marine observations and satellite altimetry derived gravity anomalies data sets have been made (Sandwell and Smith 1997; Andersen and Knudsen 1998). The reported precision ranges from 3 mGal to 14 mGal and varies as a function of geographic location. In the North Atlantic, the reported precision for the model of Sandwell and Smith (1997) is 7.6 mGal and for the KMS02 model is 5.8 mGal (Andersen and Knudsen 1998). KMS02 shows the best agreement with ship-borne gravity data and on this basis we adopted this model (KMS02) as our background model.

2.3 The geopotential model

With the recent dedicated gravimetric satellite missions CHAMP and GRACE and the in-coming GOCE mission, the long (about 200 km) wavelengths of the gravity field will be able to be accurately determined using satellite data only. Based on GRACE data, a new generation of Earth geopotential gravity field models has been derived, namely EIGEN-CG03C and EIGEN-GL04C (Förste et al. 2005; 2006) and GGM02C (Tapley et al. 2005). These models are complete to degree and order 360. The

original GGM02C model complete to order and degree 200 was extended to degree and order 360 by using the EGM96 (Lemoine et al., 1997) coefficients. In our study, these global geopotential models and EGM96 were evaluated for the ICA area, and on the basis of the comparisons (as detailed below in Section 5) the chosen model was the extended GGM02C.

2.4 The digital terrain model

There is a direct relation between the quality of a DTM (Digital Terrain Model) and the precision of estimated quantities of the gravity field such as the geoid or gravity anomalies (Forsberg 1984). The effect of DTM resolution and accuracy on the accuracy of geoid models has already been investigated for the area over the Azores (Catalão and Bos, 2008), revealing differences on the geoid of up to 3 cm rms. For the area over Iran, Kiamehr and Sjoberg (2005) have also reported differences (of up to 1 m) with respect to the geoid height from old Globe DTM to SRTM DTM. Geoid solutions, computed with rough global DTMs, are characterised by geoid degradation over rugged areas.

In this study, the objective was to construct a 100 m resolution DTM for land areas and a 500 m resolution DTM for marine areas. This was accomplished using the SRTM DTM (with 3´´ resolution) combined with medium scale maps (1:50,000 and 1:25,000). For the Azores Islands and mainland Portugal, a better vertical accuracy DTM was constructed from 1:25,000 charts of the National Army Geographic Institute. It was verified that SRTM data contain a large number of gaps which, in this study, were carefully edited and fixed with background data from older DTMs. The overall estimation of the planimetric and vertical accuracy is 20 m and 16 m, respectively, representing a 90 % confidence interval. A precise shoreline (supplied by IGP) in ETRS89 coordinates was used to uniquely define the land-sea transition for all data sets and to smooth the transition. Over marine areas, the GEBCO (General Bathymetric Chart of the Oceans, http://www.gebco.net) grid was used, and for some areas around south Portugal (including around the Azores archipelago), precise data from recent multi-beam bathymetry surveys were used.

The final DTM comprised a set of rectangular grids of 5° x 5º plus an envelope of 1° to create a two-degree overlap between adjacent blocks. For more remote effects, a continuous grid with a 0.005 degree (500 m) resolution, and covering the whole area, was constructed using all higher resolution grids. The accuracy of high resolution grids was assessed by computing the differences with the set of GPS/levelling points subsequently also used for evaluating geoid quality; the assessment resulted in a 3 m vertical accuracy (for Iberia and the Azores).

3. Gravity data processing

3.1 Computation of geopotential model contribution

A geopotential model is usually defined by a set of coefficients from degree 2 to N_{max}. At a point P the gravity anomaly is computed from the global geopotential model by:

$$\Delta g_{GGM}(\phi,\lambda,r)=\frac{GM}{r^2}\sum_{n=2}^{N_{\max}}(n-1)\left(\frac{a}{r}\right)^n\sum_{m=0}^{n}\left(\Delta C_{nm}\cos m\lambda+\Delta S_{nm}\sin m\lambda\right)P_{nm}(\sin\phi) \quad (1)$$

and the geoid height by:

$$N_{GGM}(\phi,\lambda,r)=\frac{GM}{r\gamma}\sum_{n=2}^{N_{\max}}\left(\frac{a}{r}\right)^n\sum_{m=0}^{n}\left(\Delta C_{nm}\cos m\lambda+\Delta S_{nm}\sin m\lambda\right)P_{nm}(\sin\phi) \quad (2)$$

where: (ϕ, λ, r) are the spherical (geocentric) coordinates of point P; ΔC_{nm}, ΔS_{nm} are the fully normalized geopotential coefficients of the anomalous potential; GM is the geocentric gravitational constant; a is the semi-major axis of the reference ellipsoid; P_{nm} are the fully normalized Legendre functions; γ is the normal gravity (GRS80) at point P; and N_{max} is the maximum degree of the geopotential model.

Importantly, the coordinate r must be referred to the surface of the geoid and is not known beforehand. This can be solved through an iterative procedure. A first approximation of the location of point P is given by the evaluation of Equation (2) for h=0. The first approximation for the geoid ellipsoidal

height is used in Equation (1) to compute the gravity anomaly on the geoid and also in Equation (2) to recompute the geoid undulation.

Regarding the gravity anomalies, the computation was performed point-wise on the gravity measurement location. The reduced gravity anomalies Δg_{red} were obtained by subtracting the geopotential model anomalies from the free air gravity anomalies:

$$\Delta g_{red} = \Delta g_{FA} - \Delta g_{GGM} \quad (3)$$

If the gravity anomalies determined by the global geopotential model are close to the observed gravity anomalies, it is reasonable to presume that the geopotential model is suitable to represent the long wavelength for a regional geoid model.

The last factor affecting the computation of the geoid height is the tide system, i.e., the deformation of the Earth caused by the Sun and the Moon. Different tide effects lead to different geoids. Three types of tide system are considered (Rapp et al. 1991; Basic and Rapp 1992): tide-free, where the effects of the Sun and the Moon (both direct and indirect) are removed; mean-tide, where no permanent effects are removed; and zero-tide, where the permanent direct and the periodic effects of the Sun and Moon are removed but the indirect component related to elastic deformation is retrieved. The same reasoning can be applied to the ellipsoid associated with the geoid. The effect of changing a tide system affects only the C_{20} term and does not affect the W_0 value (geoidal constant). The default C_{20} coefficient of the GGM02C geopotential model is zero tide value in accordance with the IAG resolution n. 16 of 1983, which means that the resulting geoid model is in a zero tide system. The geoid height was computed on a grid in the zero tide system in accordance with the IAG resolution, and was later converted to the mean tide system for comparison with mean sea surface heights.

3.2 Computation of topo-bathymetric effects

In order to satisfy the boundary value problem of physical geodesy, the topographic masses outside the geoid must be condensed onto it or removed. For that purpose a DTM must be used to compute the topographic effects on the measured gravity quantities. The classical terrain correction, in planar coordinates and for a constant density ρ, is given by (Forsberg 1984):

$$C_P = G\rho \int_{x_1}^{x_2} \int_{y_1}^{y_2} \int_{z_1}^{z_2} \frac{(z - h_P)}{\ell^3} dx dy dz \qquad (4)$$

where: G is the gravitational constant; ρ is the mass density; and ℓ is the distance between the computation point (x_P, y_P, h_P) and the integration point (x,y,z). The vertical integration is taken from the geoid, z_1, to the surface, z_2. The integral is evaluated over the irregularities of the topographic mass relative to a Bouguer plate passing through the computation point. In this study, the terrain correction was computed for all individual data points using the prism integration procedure implemented in the TC programme of the GRAVSOFT package (Tscherning et al. 1992). This terrain correction is added to the reduced anomalies in order to obtain the fully reduced anomalies in agreement with Helmert's second condensation method.

The shifting of masses which are above the geoid to a surface layer on the geoid in the Helmert condensation method implies, in practice, a gravity reduction and hence also a reduction in the gravity potential and a change in the geoid. This change is referred to as the indirect effect. The indirect effect of Helmert's second condensation reduction on the geoid is given in planar approximation by (Wichiencharoen 1982):

$$N_{ind} = -\frac{\pi G\rho}{\gamma} h^2(x_P, y_P) - \frac{G\rho}{6\gamma} \iint \frac{h^3(x,y) - h^3(x_P, y_P)}{s^3} dx\, dy \qquad (5)$$

where: s is the planar distance between the point P and the integration point. The topographic and bathymetric effects were computed with densities of 2670 kg m^{-3} and 1000 kg m^{-3}, respectively. The indirect effect has a maximum value of -0.68 m, at the summit of Mt Teide volcano (3718 m).

3.3 Gravity data merging and gridding

The gravity measurements obtained from different institutions and from different sources needed to be merged and integrated into a consistent data set. The merging process was executed in three steps: first, land data were analysed for temporal variations and for bias between surveys; second, land data were merged with satellite derived gravity anomalies, and a background grid thus derived; and third, the shipborne data were assimilated with the background model by least squares optimal interpolation. These steps are described below.

The background model was constructed from satellite derived gravity anomalies in the KMS02 gravity data model. A mask with the coastal line with an offshore buffer of 20 km was constructed and used to clean all satellite data inside that area on account of the data degradation characteristic of coastal regions. Land data were used to fill these blank areas and a final grid was constructed containing satellite derived gravity anomalies over sea and observed anomalies over land areas, with the same correlation distance of 10 km as used to compute the KMS02 model. The process of gridding is subject to aliasing in the presence of a high-frequency signal. With gravity data, part of this high frequency signal is due to the topography and can be removed from the original signal by removing the residual terrain model effect on the Bouguer plate. The resulting residual anomalies are given by:

$$\Delta g_{RTM} = \Delta g_{FA} - \Delta g_{GGM} - 2\pi G\rho\,(H_P - H_{ref}) + C_P \qquad (6)$$

The terrain correction C_P was calculated from the irregularities of the topography, after removal of a Bouguer plate (using Equation 4). The term $2\pi G\rho(H_P\text{-}H_{ref})$ was estimated from the irregularities of the topography with respect to a topographic reference surface of 100 km resolution, the same resolution of the geopotential model. The topographic reference surface was generated by low-pass filtering the original 100 m resolution DTM. The standard deviation of the residual gravity anomalies was reduced

from 32 mGal to 11 mGal when the GGM02C geopotential model was used and the mean value reduced to almost zero.

The gridding was performed by means of least squares collocation using residual gravity anomalies. Data were detrended prior to gridding by removing the mean value (0.11 mGal) and using a Gauss Markov covariance function model (an exponential function that decays with radial distance):

$$C(\psi) = C_0\left(1+\frac{\psi}{\alpha}\right)e^{-\frac{\psi}{\alpha}} \qquad (7)$$

where: ψ is the spherical distance; C_0 is the variance of the data; and α is the correlation length. A correlation length of 20 km was used, the value being determined from the empirical covariance function computed with the residual gravity anomalies. The computation point was the centre of a cell with a resolution of 0.025 degrees, extending from 20.0125N to 44.9875N in latitude and 39.9875W to 7.9875E in longitude and containing 1000 rows and 1920 columns.

The final step in the merging and gridding process was the merging of ship-borne data with the background gravity model. The discrepancies between the background model and the ship-borne measurements were computed and exhibit a mean value of -0.96 mGal and a standard deviation of 7.1 mGal, in agreement with the results presented for this area by Andersen and Knudsen (1998).

The unbiased residuals, associated background error covariance, and observation error model covariance were used to derive a correction surface by means of least squares optimal interpolation. The correction surface was assimilated into the background model (constructed using satellite derived gravity data) thereby yielding the best possible estimate of the gravity field. The resulting gravity model shows a misfit against the marine observations of 2.6 mGal, with a considerable recovery of the high frequency spectrum of the gravity field. Finally the geopotential model contribution was repositioned and the $2\pi G\rho(H_P-H_{ref})$ term was added, yielding Faye anomalies. It is important to note

that the removal of both effects was made point-wise, and the recovery was performed in grid format. The results for the final free air gravity anomalies are presented in Table 1.

Insert Table 1.

The gravimetric effect of the geopotential model and the residual terrain model is pronounced, reducing the gravity field variability almost three-fold from 31 mGal to 11 mGal. This is a remarkable improvement compared with earlier solutions (Catalão and Sevilla 2004) in which a residual standard deviation of 17 mGal was obtained, and reflects the high quality of the DTM used here in the RTM computation. The final grid of free-air gravity anomalies for ICA region (ICAGRA07) are depicted in Fig. 2.

4. Geoid computation

The Stokes integral for computing the geoid undulation N at an arbitrary point on the geoid can be expressed as (Heiskanen and Moritz, 1967):

$$N(\phi,\lambda) = \frac{R}{4\pi\gamma}\iint_{\sigma} S(\psi)\,\Delta g\,(\phi',\lambda')\,d\sigma \qquad (7)$$

where: Δg are the gravity anomalies referred to the geoid; $S(\psi)$ is the Stokes function; σ is the Earth's surface; R is the mean radius of the Earth; and γ is the mean normal gravity. There are two drawbacks to the direct application of this expression: first, the integral should be evaluated for the whole Earth; and second, there should be no masses outside the geoid. The former can be solved by the use of a global geopotential model removing the long wavelength component of the signal from the gravity anomalies. The latter implies that the gravity measurements must be reduced to the geoid. In this study, masses were shifted to the geoid using Helmert's second condensation reduction and the associated downward shift of the data from the topographic surface to the geoid is given

approximately by the terrain correction C_p (Equation 4). The resulting residual gravity anomalies are obtained by:

$$\Delta g_{res} = \Delta g_{FA} - \Delta g_{GGM} + C_P \tag{8}$$

where: Δg_{FA} are the observed free-air anomalies. The statistics for these residual gravity anomalies are reported in the last row of Table 1. The Stokes integral is applied to the residual anomalies

$$N_{SPFFT} = \frac{R}{4\pi\gamma}\iint_{\sigma_0} S(\psi)\left(\Delta g_{FA} - \Delta g_{GGM} + C_P\right) d\sigma \tag{9}$$

and then the low frequencies are restored as geoid undulation given by the Earth geopotential model. The final geoid undulation is given by:

$$N = N_{GGM} + N_{SPFFT} + N_{ind} \tag{10}$$

where: N_{GGM} is the geoid undulation derived from the global geopotential model; and N_{ind} (Equation 5) is the indirect effect resulting from using Helmert gravity anomalies in Stokes' formula. The long wavelength and short wavelength contributions have already been computed in Sections 3.1 and 3.2, respectively.

In this study Stokes' formula was evaluated using the spherical FFT approach (Forsberg and Sideris 1993) in which the geoid signal is obtained by a number of bandwise Fourier transformations given by:

$$N(\phi,\lambda) = \frac{R}{4\pi\gamma} F^{-1}\left\{F(S)\cdot F(\Delta g_r \cos\phi)\right\} \tag{11}$$

where: F is the two-dimensional Fourier transform; ϕ is the latitude; and S is the Stokes function.

In order to avoid distortions in the long-wavelength geoid signals caused by the local data overlapping the reference geoid data, a modified Stoke's function is used:

$$S'(\psi) = \sum_{\ell=N_{mod}}^{\infty} \frac{2\ell+1}{\ell-1} w_{\ell} \, P_{\ell}(\cos\psi) \qquad (12)$$

The cut-off modification parameter N_{mod} is, in principle, the spherical harmonic degree to which the reference field is known to be error-free and w_l is the spectral weights dependent on the error degree variances of the potential coefficient model and of the gravity anomalies (Denker et al., 1995).

Several geoid models were computed with 1-band through to 20-band spherical FFT solutions and varying the degree of the geopotential model N_{mod}. The solutions were compared with mean sea surface data and the best agreement was obtained with a Wong-Gore modification with N_{mod} = 120, i.e., when considering all geopotential coefficients. Fig. 3 shows a shaded relief image of the final geoid height model, ICAGM07 (Iberia Canary Azores Geoid Model-07). The geoid heights range from a low of -5.7 m in the south-west mid-Atlantic to a high of 64.4 m to the north of the Azores. Most of the geoid signals are correlated with tectonic features.

5 Geoid accuracy assessment

The validation and accuracy assessment of the ICAGM07 gravimetric geoid model over sea was made using mean sea surface (MSS) and mean dynamic topography (MDT) and over land was made using GPS/levelling data. The comparison can be achieved, on land, by applying the simple relationship between the ellipsoidal height h (given by GPS), the geoid model N, and the orthometric height H:

$$h = H + N \qquad (13)$$

Over sea the equivalent relation should be given by:

$$MSSH = N + MDT \quad (14)$$

where: MSSH is the ellipsoidal mean sea surface height; and MDT is the mean dynamic topography.

Due to several factors, including datum inconsistencies inherent to each vertical reference system, distortions in the height data (ellipsoidal and orthometric) and long wavelength geoid errors, the above expressions are not exact and must not be directly applied. In addition, the geopotential model used for the geoid computation does not have degree zero because the Earth's mass and potential are poorly determined. This effect on the geoid corresponds to a bias that must be determined globally. Furthermore, the orthometric heights are referred to a local reference system connected to a tide gauge. Therefore, a transformation is necessary. Generally a 4-parameter affine datum shift transformation (with no rotations) is used to remove datum shift parameters and long wavelength geoid errors, detected as a tilt. The most common 4-parameter model used is the simplified model provided by Heiskanen and Moritz 1967:

$$(h-H)-N = N_{geom} - N_{grav} = \Delta X \cos\phi\cos\lambda + \Delta Y \cos\phi\sin\lambda + \Delta Z \sin\phi + N_0 \quad (15)$$

where: (h-H)-N can be substituted by (MSSH-MDT)-N over sea; ΔX, ΔY, and ΔZ are the datum shift parameters; and N_0 is a global geoid bias close to the missing zero degree term in Stokes' formula. Higher order corrector surfaces will lead to a better adjustment of geoid and ellipsoidal height, but will also absorb GPS and network error into the model.

The data used for comparison over sea areas were the MSS data in CLS01 (Hernandez and Schaeffer 2000) and GSFC00.1 (Koblinsky et al. 1999). The CMDT Rio05 (Rio and Hernandez, 2004) oceanographic MDT data were also used for the comparison. The CLS01 MSS was determined with TP data (from 1993-1999, cycles 11-280), ERS-1 data (from 1993-1999, 64 cycles), Geosat data (from

1987-1988, cycles 1-44), and ERS-1 geodetic phase data (1994-1995). The GSFC00.1 MSS was computed by combining multi-mission satellite altimeter data with six years of T/P data (Cycles 11 to 232), multiple years of ERS-1/2 35-day repeat cycle data, Geosat ERM data (Cycles 1 to 41), Geosat GM data, and ERS-1 168-day data. The CLS CMDT Rio05 was computed for the 1993-1999 period, by means of a multi-variate analysis using hydrographic data, surface drifter velocities, and altimetry. The estimated model is based on both the CLS01 MSS / EIGEN-GRACE 03S geoid and Levitus '98 climatology data (referenced to 1500 dbar).

Over land, a total of 1646 geodetic marks of known orthometric and ellipsoidal height were used for the geoid evaluation. The orthometric heights were determined by trigonometric levelling on the Azores and Madeira Islands and by spirit levelling elsewhere. The global estimation for both techniques is about 1 cm for spirit levelling and 10 cm for trigonometric levelling. Ellipsoidal heights were determined from GPS observations. The observation period for GPS surveys was 2 hours minimum for each benchmark, with an observation rate of 30 s, connected to the ETRS89 reference system for Iberia. For the islands, the orthometric heights are referred to the local vertical datum and the ellipsoidal heights (h) are referred to the ITRF94 reference frame for the Azores archipelago, and were surveyed between 1995 and 2000. For the Canary Islands, the ITRF89 was adopted, for which surveys took place in 2003 and 2004.

The first comparison was aimed at selecting the best-fit geopotential model for the ICA region. Four geopotential models were evaluated: the EGM96, GGM02C, CG03C, and GL04C. Four gravimetric geoid models were computed, each with a different geopotential model used in the remove-restore procedure. The evaluation was made with CLS01 MSS data and Rio05 MDT data over sea (570607 data points) and with GPS/levelling data over Iberia (Portugal, 135 data points and Spain, 317 data points). The MSS was converted from the mean tide system to the zero tide system (see Eakman (1989) and Rapp et al. (1991)) in order to be comparable with the geoid. The statistics of the comparison are summarized in Table 2, which presents the mean residual and standard deviation with

respect to the mean. The geoid model computed with GGM02C (third row of Table 2) agrees with GPS/levelling data to better than 12 cm for Iberia and for that area is clearly superior to the geoids computed using other geopotential models. Over sea, the agreement is essentially equivalent between models. The regional solution (third row of Table 2) is a considerable improvement with respect to the global geopotential solution (GGM02C, first row of Table 2), increasing the relative accuracy from 21 cm to 8 cm over sea and from 27 cm to 12 cm over land (Spain). Therefore, GGM02C was used as the reference geopotential model for the ICAGM07 geoid model.

Insert Table 2

In order to obtain an external, independent verification of the accuracy of the ICAGM07 geoid model over sea, two different MSSs determined from satellite altimetry and the Rio05 oceanographic MDT were used. The MSSs are in the mean tide system and were converted to the zero tide system in order to be compared with the geoid. Un-modelled datum incoherencies were minimised with a 4-parameter affine datum shift transformation parameterized as a bias and a tilt. The residual statistics applying to each surface are presented in Table 3.

Insert table 3

The ICAGM07 geoid model has a relatively good agreement with the MSS with a mean residual of 23 cm and a relative accuracy of 15 cm. The bias between both surfaces may be due to the missing zero degree harmonic term of the disturbing potential or may represent the mean value of the MDT. The tidal correction contributes to the reduction of the standard deviation by 2 cm (Table 3), removing a plane-like tilt dependence on latitude. The mean residual value is not changed. The highest residuals are close to the shoreline and between islands, which can be explained by satellite altimetry degradation close to land areas and consequently reflected in the MSS. The difference between the geoid and the MSSH is likely to reproduce the MDT. The misfit of the derived MDT to an

oceanographic MDT (Rio05) is 8.1 cm. Again, the highest values are still close to the shoreline and in the inter-island areas. If these measurements close to land are not considered, the relative accuracy reduces to 6.1 cm. Fig. 4 reveals a periodic (~5 degrees) longitudinal effect in the residual pattern and also a circular effect over the Canary archipelago. Both effects seem to be related to the geopotential model. The first can be explained by the zonal harmonic dependence on the satellite data. The second effect represents an aliasing problem of the model unable to reproduce the high frequency gravity signal of Tenerife Island. This is a finding that must be taken into consideration in future releases of the geopotential model.

The GSFC00.1 MSS and the CLS01 MSS are virtually identical in the ICA region. In fact, the difference has only 2.8 cm on the standard deviation with a bias of 3 cm (Table 3). The adjustment with a 4-parameter transformation shows that there is no improvement in the geoid model accuracy. This means that there is no significant tilt or datum shift between altimeter data and the geoid, but a considerable bias of -1.95 (due to the MDT) was detected and recovered into the adjusted geoid model.

The results demonstrate that the ICAGM07 model appears to be one of the best geoid solutions for the Atlantic, with an agreement in the order of 8 cm with independent models derived from satellite altimetry and oceanographic data. This agreement is much less than the typical values of 14 cm obtained previously (Vergos and Sideris 2003; Vergos et al. 2005) although is similar to those presented in the GOCINA project (Knudsen et al. 2006).

Over land, a total of 1646 geodetic marks with known orthometric and ellipsoidal height were used for the geoid evaluation. Most of these geodetic marks are in the Canary archipelago (932) and the remaining are distributed homogeneously throughout the other islands (see Table 4). Although the GPS/levelling pair of observations is likely to represent the geoid, their dependence to a local vertical datum, defined by the mean sea level over a period of time, could render these observations useless.

However, the GPS/levelling data are the only observations able to be used to control the gravimetric geoid on land, and the local datum effect can be reduced to a (local) bias. Furthermore, these observations provide a measure of the geoid performance for transforming ellipsoidal to orthometric heights, which is the first application for geoid heights on land. The evaluation and analysis over land was divided into the archipelagos (Macaronesian Islands) and the Iberian peninsula. The geological framework is different between these areas and the geodetic instrumentation and techniques used for height computation were also different.

Insert table 4

The standard deviation was computed for each island and a range of values between 6.5 cm on Faial and 29.5 cm on Tenerife Islands was determined. This is the best way to assess the precision of the geoid, but in this particular case (the Azores and Canary Islands) the geoid residual standard deviation must not be viewed as purely geoid error but as containing levelling and GPS position errors and surface vertical deformation as well. Particularly in the Azores, each island has experienced different tectonic and volcanic dynamics during the lengthy period between the trigonometric survey (1940-1950) and the GPS survey (1995-1997). In fact, on these active islands, the residuals between the gravimetric and geometric geoid may be due to local vertical deformation in addition to the expected observational and modelling errors. The mean residual between the gravimetric geoid and the GPS/levelling vertices varies in the Canary archipelago from 0.89 m on La Palma and -1.17 m on Tenerife, and in the Azores archipelago from -0.44 m on S. Miguel to -0.64 on Pico. These mean residual values may be interpreted as the vertical datum shift relative to the geoid surface given by the ICAGM07 model. In the Canary archipelago, the obtained values are unrealistic at about 2 m vertical difference between two islands. As discussed above, over sea there are also large discrepancies around the Canary archipelago with a concentric wave type effect attributed to the GGM02C global geopotential model. This effect was also seen previously in the EGM96 geopotential model.

Finally, a locally adjusted solution was determined for each island using a 4-parameter model. This geoid solution will be useful for local transformation between orthometric and GPS heights. The geoid residual standard deviation was considerably reduced, from a maximum of 22 cm on La Palma to a minimum of 2.2 cm on Faial. This latter value is very promising for enabling the transformation of old orthometric heights to ellipsoidal heights, allowing the determination of time series of vertical deformations. The same reasoning applies to the other islands but with less precision. Over Faial, the geoid model performs much better than on other islands partly because of the high quality and density of gravity measurements, about 1 point per km^2, but also (and mainly) because of the recent orthometric heights used in the external evaluation. The external evaluation performed on the other islands includes not only the geoid errors but also the old orthometric errors and possible temporal vertical deformation. On a regional scale, the results of Table 4 provide the expected precision for transforming orthometric to GPS heights.

For Iberia, ICAGM07 was evaluated with 452 GPS/ levelling marks. The geodetic networks in Portugal and Spain were treated separately due to their respective different vertical datums. For Portugal the vertical datum is Cascais (on the Atlantic coast) and for Spain is Alicante (on the Mediterranean coast). Notwithstanding the different geodetic networks and different countries, the standard deviation is similar for both areas, both before and after the removal of datum inconsistencies, although the mean residual has a difference of 16 cm. This bias may be viewed as an offset of 16 cm between the vertical datum for Portugal and Spain and is close to the 17.1 cm obtained from the EUVN, revealing a very good precision of this geoid model with respect to vertical data unification. An absolute comparison was also made with earlier geoid models: the GGM02C geopotential model; the EGG97 model (Denker et al. 1995); and the IGG2005 model (Corchete et al. 2005). The statistics of the comparison are summarized in Table 5. For Portugal, ICAGM07 is considerably better than other models, most probably due to the use of a precise DEM for terrain effects computation. However, for Spain, the EGG97 solution reveals a slightly better fit with

GPS/levelling data. After a 4-parameter adjustment to the local GPS/levelling data, the standard deviation of the residuals reduces by about 1 cm in both territories.

Insert table 5

7. Summary and conclusion

This paper has summarized the data preparation and methodology used in the computation of a new gravimetric geoid model (ICAGM07) for the North-east Atlantic Ocean, and Iberia, Canary, and Azores land areas.

The gravity data were obtained from several databases and were compiled, edited, and validated. Particular care was taken in offshore areas to guarantee the continuous transition of gravity and DEM /bathymetry from land to sea. The merging of satellite derived gravity anomaly and marine measurements was performed using optimal interpolation. Different geopotential model solutions were evaluated and it was found that the GGM02C geopotential model, augmented to degree 360 using EGM96, fits the local gravity field slightly better than other geopotential models. A new DTM, the computed SRTM, and local high precision DEMs reduced the gravity field variability almost three times from 32 mGal to 11 mGal. This is a remarkable improvement on earlier solutions, and reflects the high quality of the DTM used in the RTM computation.

The geoid was computed using the remove-restore spherical FFT method using gravity data reduced by Helmert's second condensation method. The long wavelengths from the geopotential model were subsequently repositioned and the indirect effect added. Geoid accuracy was evaluated both over sea and over land. The marine evaluation was achieved by comparing the geoid with an oceanographic geoid computed from CLS01 mean sea surface and Rio05 mean dynamic topography (MSSH-MDT). The comparison indicates an overall relative accuracy of 8 cm relative to a mean of 23 cm, and no tilt was detected between these surfaces. A periodic longitudinal effect in the residuals was detected and a

circular effect over the Canary archipelago, with both effects seemingly related to the geopotential model. The periodic effect is explained by the zonal harmonic dependence on the satellite data, while the circular effect is an aliasing problem of the model which renders it unable to reproduce the high frequency gravity signal of Tenerife Island. These findings must be taken into consideration in future releases of the geopotential model.

Over land, a total of 1646 geodetic vertices with known orthometric and ellipsoidal heights were used for the evaluation of the geoid. The standard deviation was computed for each island and a range of values between 2.2 cm on Faial and 22 cm on La Palma Islands was determined. Over Iberia, the standard deviation was 9cm and 10cm for Portugal and Spain, respectively. The mean residual between the gravimetric geoid and the GPS/levelling vertices was determined for each island and Iberia, and interpreted as the vertical datum shift relative to the present-day mean sea surface. The relative bias between local vertical data was assessed and a maximum relative vertical datum shift, of 2.06 m, was determined between La Palma and Tenerife Islands. This large relative bias was attributed to the global geopotential model.

Overall, significant progress has been made towards the computation of a high precision gravity model and gravimetric geoid for the north-Atlantic area, and towards the unification of the 14 local vertical datums currently in use. This geoid model, ICAGM07, provides a significant improvement over existing geoid models for this area. The improvement is especially significant over sea and in mountain areas such as the Pyrenees, North Portugal, and the Azores archipelago. ICAGM07 will allow further studies on characteristics of the regional ocean circulation and on earth dynamics (e.g., isostatic compensation, admittance computation, and dynamic processes in the mantle).

Acknowledgements

We acknowledge IGP (Instituto Geográfico Português) and IGN (Instituto Geográfico Nacional) for supplying the gravity and GPS data for the Portuguese and Spanish mainlands, respectively. This work was funded by GRICES/CSIC and also by FCT (Portuguese Foundation for Sciences and Technology) through KARMA (POCI/CTE-GIN/57530/2004) projects.

References

Andersen O.B., Knudsen P., Kenyon S., Trimmer R., 1999. Recent improvement in the KMS global marine gravity field. Bollettino Geofisica Teorica ed Applicata, 40, 369–377.

Andersen O.B., Knudsen P. 1998. Global marine gravity field from ERS-1 and Geosat geodetic mission altimetry. J. Geophys. Res., 103(C4), 8129–8137.

Arabelos D., Spatalas S.D., Tziavos I.N., Sevilla M.J., Rodríguez G., de Toro C., Catalão J., Calvão J., 1999. A new high resolution geoid for the north-east Atlantic. Bolletino di Geofisica Teorica ed Applicata, Vol.40: 411-420.

Bamler R., 1999. The SRTM Mission: A world-wide 30 m resolution DEM from SAR Interferometry in 11 days. In: D. Frisch and R. Spiller (eds.): Photogrammetric week 99, Wichman verlag Heidelberg: 145-159.

Basic T., Rapp R.H., 1992. Oceanwide prediction of gravity anomalies and sea surface heights using Geos-3, Seasat, and Geosat altimeter data and ETOPO5U bathymetric data. Dept. of Geodetic Science and Surveying, Rep. No. 416, The Ohio State University, Columbus, Ohio.

Catalão J., 2006. Iberia-Azores Gravity Model (IAGRM) using multi-source gravity data. Earth, Planets, Space, 58, 277–286.

Catalão J., Sevilla M., 1998. Geoid studies in the north-east Atlantic (Azores-Portugal). In Geodesy on the Move, Eds. R. Forsberg, M. Feissel R. Dietrich, ISBN 3-540-64605-1, Springer-Verlag. Berlín, 269-274,

Catalão J., Sevilla M., 1999. The effect of high precision bathymetric model on geoid computation. IGS Bulletin, 10: 91-99.

Catalão J., Sevilla M., 2004. Inner and minimum constraint adjustment of marine gravity data. Computers and Geosciences, Vol. 30, Issues 9-10: 949-957, doi: 10.1016/j.cageo.2004.06.004

Catalão J., Bos M., 2008. Sensitivity analysis of the gravity geoid estimation: A case study on the Azores plateau. Physics of the Earth and Planetary Interiors, doi:10.1016/j.pepi.2008.05.010.

Corchete V., Chourak M., Khattach D., 2005. The high-resolution gravimetric geoid of Iberia: IGG2005. Geophysical Journal International, 162: 676-684.

Denker H., Barriot J.P., Barzaghi R., Forsberg R., Ihde J., Kenyeres A., Marti U., Tziavos I.N., 2005. Status of the European Gravity and Geoid Project EGGP. In International Association of Geodesy Symposia. Gravity, Geoid and Space Missions GGSM 2004 IAG International Symposium Porto, Portugal August 30 – September 3, 2004, Ed. Christopher Jekeli, Luisa Bastos and Joana Fernandes, DOI 10.1007/3-540-26932-0_22, 125-130.

Denker H., Behrend D., Torge W., 1995. The European gravimetric quasigeoid EGG95. BGI Bull D' Inf 77 (Toulouse) IGeS Bull 4 (Milano), 3-11.

Eakman M., 1989. Impacts of Gedynamic Phenomena on Systems for height and gravity. Bulletin Geodesique, 63: 281-296.

Featherstone W.E., Kirby J.F., Kearsley A.H.W., Gilliland J.R., Johnston G.M., Steed J., Forsberg R., Sideris M.G., 2001. The AUSGeoid98 geoid model of Australia: data treatment, computations and comparisons with GPS-levelling data. Journal of Geodesy, 75: 313-330.

Fernandes M.J., Gidskehaug A., Solheim D., Mork M., Jaccard P., Catalao J., 1998. Gravimetric and Hydrographic campaign in Azores.In Proceedings of the I Luso-Spanish Assembly in Geodesy and Geophysics, Almeria, Spain, 9–13 Feb., University of Almeria, 113.

Fernandes M.J., Bastos L., Catalão J., 2000. The role of dense ERS altimetry in the determination of the marine geoid in Azores. Marine Geodesy, Vol. 23, N. 1, 1-16.

Fernandes M.J., Barbosa S., Lazaro C., 2006. Impact of Altimeter data Processing on sea level studies. Sensors, 6: 131-163.

Forsberg R., 1984. A study of terrain reductions, density anomalies and geophysical inversion methods in gravity field modelling. Dep. Of Geodetic Science and Surveying, Rep. No. 355, The Ohio State University, Columbus, Ohio,

Forsberg R., Sideris M.G., 1993. Geoid computations by the multi-band spherical FFT approach. Manuscripta geodaetica, 18: 82-90.

Forsberg R., Olesen A., Bastos L., Gidskehaug A., Meyer U., Timmen L., 2000. Airborne geoid determination, Earth Planets Space, 52, 863–866.

Forsberg R., Olesen A., Vest A., Solheim D., Hipkin R., Omang O., Knudsen P., 2004. Gravity field improvements in the North Atlantic region. Proc. Second International GOCE User Workshop “GOCE the geoid and Oceanography”, ESA-ESRIN, Frascati, Italy, 8-10 March 2004 (ESA SP-569, June 2004).

Forsberg R., Skourup H., 2005. Arctic Ocean Gravity, Geoid and Sea-ice Freeboard Heights from ICESat and GRACE. Geophysical Research Letters, vol. 32, L21502, 2005

Förste C., Flechtner F., Schmidt R., Meyer U., Stubenvoll R., Barthelmes F., König R., Neumayer K.H., Rothacher M., Reigber C.H., Biancale R., Bruinsma S., Lemoine J.M., Raimondo J.C., 2005. A New High Resolution Global Gravity Field Model Derived From Combination of GRACE and CHAMP Mission and Altimetry/Gravimetry Surface Gravity Data. Poster presented at EGU General Assembly 2005, Vienna, Austria, 24-29, April 2005.

Förste C., Flechtner F., Schmidt R., König R., Meyer U., Stubenvoll R., Rothacher M., Barthelmes F., Neumayer H., Biancale R., Bruinsma S., Lemoine J.M., Loyer S., 2006. A Mean Global Gravity Field Model from the Combination of Satellite Mission and Altimetry/Gravmetry Surface Data - EIGEN-GL04C. Geophysical Research Abstracts, Vol. 8, 03462.

Fotopoulos G., Kotsakis C., Sideris M.G., 2000. A New Canadian Geoid Model in Support of Levelling by GPS. Geomatica, Vol.54, No.1, 53-62.

Gitlein O., Denker H., Müller J., 2004. Local geoid determination by the spectral combination method. In: IAG Internat. Symp. "Gravity, Geoid and Space Missions - GGSM2004", Porto, Aug. 30 - Sept. 3, 2004.

Hernandez F, Schaeffer P 2000. Altimetric Mean Sea Surfaces and Gravity Anomaly maps inter-comparisons. Rapport n. AVI-NT-011-5242-CLS, édité par CLS, Ramonville St Agne. 48.

Hwang C., Hsiao Y.S., Shih H.C., Yang M., Chen K.H., Forsberg R., Olesen A.V., 2007. Geodetic and geophysical results from a Taiwan airborne gravity survey: Data reduction and accuracy assessment, J. Geophys. Res., 112, B04407, doi:10.1029/2005JB004220.

Heiskanen W.A., Moritz H., 1967. Physical Geodesy, W. H. Freeman and Company, San Francisco.

Kern M., Schwarz P.,, Sneeuw N., 2003. A study on the combination of satellite, airborne, and terrestrial gravity data, Journal of Geodesy, 77, 217–225, DOI 10.1007/s00190-003-0313-x.

Kiamehr R., 2006. A strategy for determining the regional geoid by combining limited ground data with satellite-based global geopotential and topographical models: a case study of Iran. J Geod 79: 602–612. DOI 10.1007/s00190-005-0009-5.

Kiamehr R., Sjoberg L.E., 2005. Effect of the SRTM global DEM on the determination of a high-resolution geoid model: a case study in Iran. J Geod 79: 540–551. DOI 10.1007/s00190-005-0006-8

Knudsen P., Andersen O., et al. 2006. Geoid and Ocean Circulation in the North Atlantic, Final report. Danish National Space Center, Technical Report no. 5, 2006.

Koblinsky et al., 1999. NASA Ocean Altimeter Pathfinder Project, Report 1: Data Processing Handbook, NASA/TM-1998-208605, April, 1999.

Kuroishi Y., Ando H., Fukuda Y., 2002. A new hybrid geoid model for Japan, GSIGEO2000. Journal of Geodesy, 76, 428-436, DOI 10.1007/s00190-002-0266-5.

Klees R., Tenzer R., Prutkin I., Wittwer T., 2007. A data-driven approach to local gravity field modeling using spherical radial basis functions. J Geod DOI 10.1007/s00190-007-0196-3.

Kol M., Vasconcelos M., 2000. Adensamento gravimétrico em Portugal Continental: Estudos e aplicações. In: Actas da II Conferência Nacional de Cartografia e geodesia, 23-24 Setembro 1999, Luso, Portugal, 303-310.

Lemoine F.G. at al., 1997. The development of the NASA GSFC and NIMA Joint Geopotential Model, in Proceedings of the International Symposium on Gravity, Geoid and Marine Geodesy, GRAGEOMAR, edited by J. Segawa, H. Fujimoto, and S. Okubo, The University of Tokyo, Tokyo, Sept. 30–Oct. 5, Springer-Verlag, 461–469.

Miranda J.M., Mendes-Victor L.A., Simões J., Luís J., Matias L., Shimamura H., Shiobara H., Nemoto H., Mochizuki H., Hirn A., Lépine J., 1998. Tectonic setting of the Azores Plateau deduced from a OBS survey, Marine Geophysical Researches, 20 (3), 171-182.

Prutkin I., Klees R., 2007. On the non-uniqueness of local quasi-geoids computed from terrestrial gravity anomalies. J Geod DOI 10.1007/s00190-007-0161-1, 2007.

Rapp R.H., Nerem R.S., Shum C.K., Klosko S.M., Williamson R.G., 1991. Consideration of Permanent Tidal Deformation in the Orbit determination and data analysis fort he Topex/Poseidon Mission, NASA TM 100775, Goddard Space Flight Center, Greenbelt, MD, 1991

Reigber C.H., Luehr H., Schwintzer P., 2002. CHAMP Mission Status. Advances in Space Research, 30 (2): 129-134.

Rio M.H., Hernandez F., 2004. A mean dynamic topography computed over the World Ocean from altimetry in situ measurements and a geóide model. J. Geophysical Research, 109, C12032, doi:10.1029/2003JC002226.

Rodriguez-Velasco G., Sevilla M.J., Toro C., 2002. Dependence of mean sea surface from altimeter data on the reference model used, Marine Geodesy, 25, 289–312, DOI:10.1080/01490410290051590.

Sandwell D., Smith W.H.F., 1997. Marine gravity anomaly from Geosat and ERS1 satellite altimetry, J. Geophys. Res., 102(B5), 10039–10054.

Scheinert M., Müller J., Reinhard D., Damaske R., Damm V., 2007. Regional geoid determination in Antarctica utilizing airborne gravity and topography data. Journal of Geodesy, doi: 10.1007/s00190-007-0189-2.

Schmidt M., Kusche J., 2005. Muliresolution representation of a regional geoid from satellite and terrestrial gravity data. GGSM 2004 Porto, 167-170.

Sevilla M., 1997. A high-resolution gravimetric geoid in the Strait of Gibraltar. Journal of Geodesy, Vol 71 Nº 7, 402-410.

Sevilla M.J., Ramírez D., Sánchez F., 1997. Metodología para la creación de bases de datos gravimétricos fiables. Métodos clásicos, gráficos y digitales. Topografía y Cartografía, Vol. XIV Nº 79, pp. 2-19 and Nº 80, 2-18.

Serpas J.G., Jekeli C., 2005. Local geoid determination from airborne vector gravimetry. Journal of Geodesy, 78, 577-587, DOI 10.1007/s00190-004-0416-z

Sjöberg L., 2005. A discussion on the approximations made in the practical implementation of the remove–compute–restore technique in regional geoid modeling. J Geod. 78: 645–653
DOI 10.1007/s00190-004-0430-1.

Smith D.A., Milbert D.G., 1999. The GEOID96 high-resolution geoid height model for the United States. Journal of Geodesy, 73:219-236.

Tapley B., Ries J., Bettadpur S., Chambers D., Cheng M., Condi F., Gunter B., Kang Z., Nagel P., Pastor R., Pekker T., Poole S., Wang F., 2005. GGM02 – An improved Earth gravity field model from GRACE. Journal of Geodesy, 79 (8), 467-478.

Timmen L., Bastos L., Forsberg R., Gidskehaug A., Meyer U., 2002. Airborne Gravity Field Surveying for Oceanography, Geology and Geodesy—Experiences from AGMASCO, in IAG Symposia, Volume 121, Springer Verlag.

Tscherning C.C., Forsberg R., Knudsen P., 1992. The GRAVSOFT package for geoid determination. Proc. 1st Continental Workshop on the Geoid in Europe, Research Institute of Geodesy, Cartography and Topography, Prague, 327-334.

Tziavos I.N., Vergos G.S., Kotzev V., Pashova L., 2005. Mean Sea Level and Sea Level Variation Studies in the Black Sea and the Aegean Gravity, Geoid and Space Missions GGSM 2004 IAG International Symposium Porto, Portugal August 30 – September 3, 2004, 254-259, 10.1007/3-540-26932-0_44.

Vergos G.S., Sideris M.G., 2003. Estimation of High-Precision Marine Geoid Models Offshore Newfoundland, Eastern Canada. 3rd Meeting of the International Gravity and Geoid Commission (IGGC), Tziavos (ed.), Gravity and Geoid 2002 - GG2002, 126-131.

Vergos G.S., Tziavos I.N., Andritsanos V.D., 2005. Gravity data base generation and geoid model estimation using heterogeneous data. IAG international Symposium, ed. Jekeli, C., Bastos, L., Fernandes, J.M., Gravity, Geoid and Space Missions-GGSM04.

Wichiencharoen C., 1982. The indirect effects on the computation of geoid undulation. Rep. 336, Department of Geodetic Science and Surveying, The Ohio State University, Columbus.

Table Captions

Table 1. Statistics for the gravity anomalies, in mGal (10^{-5}m/s^2). FA is the measured free-air gravity anomalies; Cp is the terrain correction; and RTM is the residual terrain model correction. GGM02C was augmented with EGM96 for degrees 201-360.

Table 2. Statistics of the differences between the gravimetric geoid computed with different geopotential models and the oceanographic geoid and GPS/levelling geometric geoid. The first line indicates the difference for the GGM02C geopotential model. Values are in m.

Table 3. Statistics for the comparison of the ICAGM07 geoid model with mean sea surface minus mean dynamic topography (MSSH-MDT) and conversion from mean tide system to zero tide. The statistics are referred to the CLS01 and GSFC00.1 mean sea surface models and the MDT Rio5 mean dynamic topography model. The last line is the relative accuracy after 4-parameter adjustment. Values are in m.

Table 4. Statistics for the comparison of ICAGM07 with GPS/levelling data over 12 islands. The last column is the relative accuracy after long wavelength removal determined from a local 4-parameter adjustment. Values are in m.

Table 5. Statistics for the comparison of ICAGM07 with GPS/levelling data over Iberia (Portugal and Spain). Accuracy evaluations of other geoid models (ICC2005 and EGG97) are also reported. The last column is the relative accuracy after long wavelength removal determined from a local 4-parameter adjustment. Values are in m.

Table 1.

Gravity anomalies (mGal)	Mean	Std	Min	Max
Δg_{FA}	9.56	31.91	-244.00	488.81
$\Delta g_{FA} - \Delta g_{GGM}$	0.06	15.92	-304.16	347.12
$\Delta g_{FA} - \Delta g_{GGM} - 2\pi G\rho\,(H_P - H_{ref}) + C_P$	0.11	11.21	-283.09	117.86
$\Delta g_{FA} - \Delta g_{GGM} + C_P$	0.25	15.96	-288.79	384.31

Table 2.

	MSS_{CLS01}-MDT_{Rio05}+ tide		GPS/levelling Portugal		GPS/levelling Spain	
	mean	Std	mean	std	mean	Std
N_{GGM02C}	-0.97	0.212	-0.89	0.222	-1.13	0.275
$N_{SPFFT} + N_{EGM96} + N_{ind}$	-1.21	0.097	-0.76	0.111	-0.88	0.167
$N_{SPFFT} + N_{CGM02C} + N_{ind}$	-1.21	0.082	-0.86	0.103	-1.02	0.117
$N_{SPFFT} + N_{CG03C} + N_{ind}$	-1.19	0.092	-0.86	0.132	-1.00	0.154
$N_{SPFFT} + N_{GL04C} + N_{ind}$	-1.21	0.082	-0.90	0.116	-1.02	0.136

Table 3.

$N = N_{SPFFT} + N_{GGM02C} + N_{ind}$	mean	Std	min	max
MSSH(CLS01) – N	0.23	0.154	-0.77	1.35
MSSH(CLS01) + TideCorr – N	0.23	0.135	-0.82	1.32
MSSH(CLS01) + TideCorr - MDT (Rio05) – N	-1.21	0.082	-2.29	-0.11
MSSH(GSFC00.1) + TideCorr - MDT (Rio05) - N	-1.95	0.081	-2.99	-0.88
MSSH(CLS01) – MSSH(GSFC00.1)	0.03	0.028		
After bias+Tilt correction				
MSSH(CLS01) - MDT (Rio05) + TideCorr - N	0.0	0.081	-1.09	1.11

Table 4.

(mGal)	Arch	#	Mean	std	min	max	Std (4-param)
S. Miguel	Az	77	-0.44	0.258	0.102	1.057	0.125
Faial	Az	33	-0.60	0.065	-0.720	-0.502	0.022
Pico	Az	55	-0.64	0.196	-1.058	-0.297	0.125
Terceira	Az	61	-0.56	0.111	-0.837	-0.211	0.090
Lanzarote	Cn	127	-0.04	0.091	-0.218	0.218	0.069
Hierro	Cn	77	0.35	0.095	0.122	0.534	0.067
La Palma	Cn	125	0.89	0.242	0.001	1.664	0.223
Gomera	Cn	92	-0.30	0.146	-0.576	0.017	0.076
Tenerife	Cn	160	-1.17	0.295	-1.712	-0.573	0.165
Gran Canaria	Cn	213	0.10	0.161	-0.393	0.509	0.106
Fuerteventura	Cn	138	0.00	0.110	-0.366	0.273	0.083
Madeira	Md	36	-0.19	0.146	-0.44	0.091	0.133

Table 5.

	#	mean	std	min	max	Std (4-param)
Portugal Mainland						
GGM02C	135	-0.89	0.222	-1.415	-0.307	0.19
EGG97	135	-0.41	0.225	-0.912	0.090	0.16
ICC2005	135	-0.37	0.234	-0.869	0.547	0.21
ICAGM07	135	-0.86	0.095	-1.087	-0.518	0.08
Spain Mainland						
GGM02C	317	-1.13	0.275	-1.928	-0.237	0.26
EGG97	317	-0.54	0.109	-1.098	-0.305	0.10
ICC2005	317	-0.41	0.234	-1.363	0.222	0.22
ICAGM07	317	-1.02	0.117	-1.325	-0.398	0.10

Figure Captions

1. Gravity data distribution across the ICA area. The area includes in the north-east the Iberian peninsula (Portugal and Spain) and the Mediterranean sea, in the south-east Africa (with almost no gravity data), and in the remaining area the Atlantic Ocean and the Azores and Canary archipelagos.

2. Final free-air gravity anomalies for the North-East Atlantic, Iberia, and Macaronesian Islands, derived from marine, land, and satellite altimetry. Colour scale is in mGal.

3. Gravimetric geoid model (ICAGM07) of the North-East Atlantic, Iberia, and Macaronesian Islands. Contours are in m.

4. Differences between the gravimetric geoid and the oceanographic geoid computed from MSSH-MDT surfaces. The meridional set of stripes and a circular shape around the Canary archipelago are effects attributed to the geopotential model.

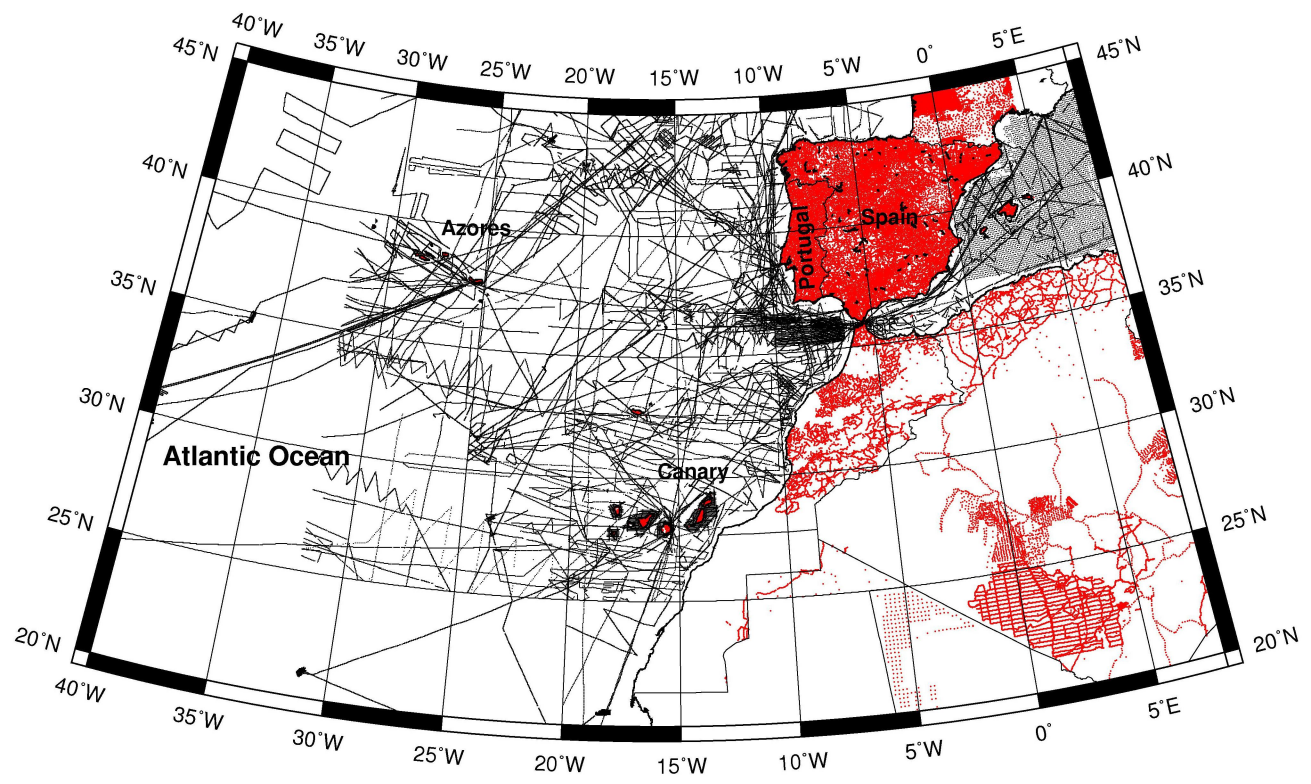
40°W
35°W
30°W
25°W
20°W
15°W
10°W
5°W
0°
5°E
45°N
40°N
35°N
30°N
25°N
20°N
Azores
Portugal
Spain
Atlantic Ocean
Canary

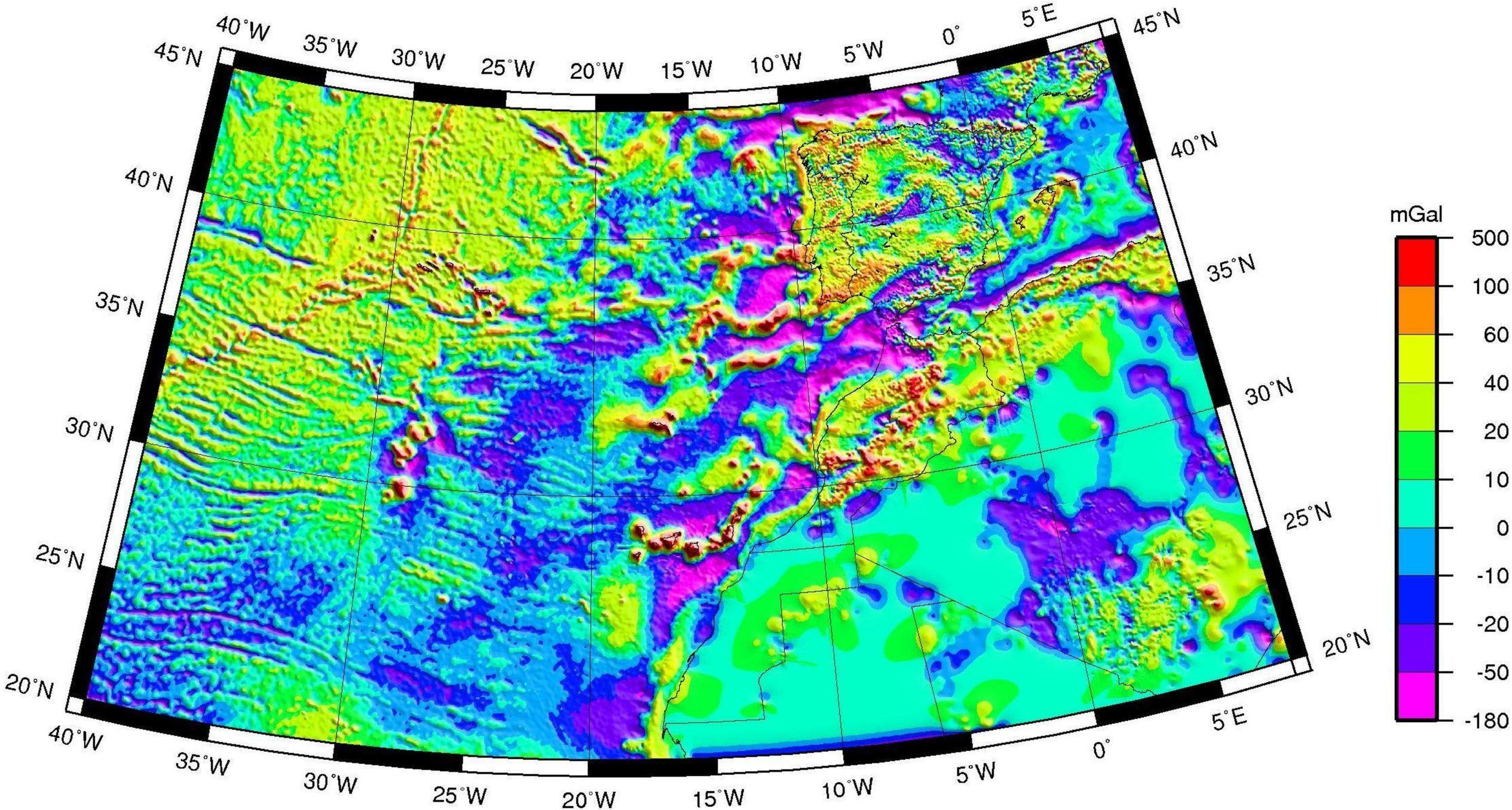
40°W
35°W
30°W
25°W
20°W
15°W
10°W
5°W
0°
5°E
45°N
40°N
35°N
30°N
25°N
20°N
mGal
500
100
60
40
20
10
0
-10
-20
-50
-180

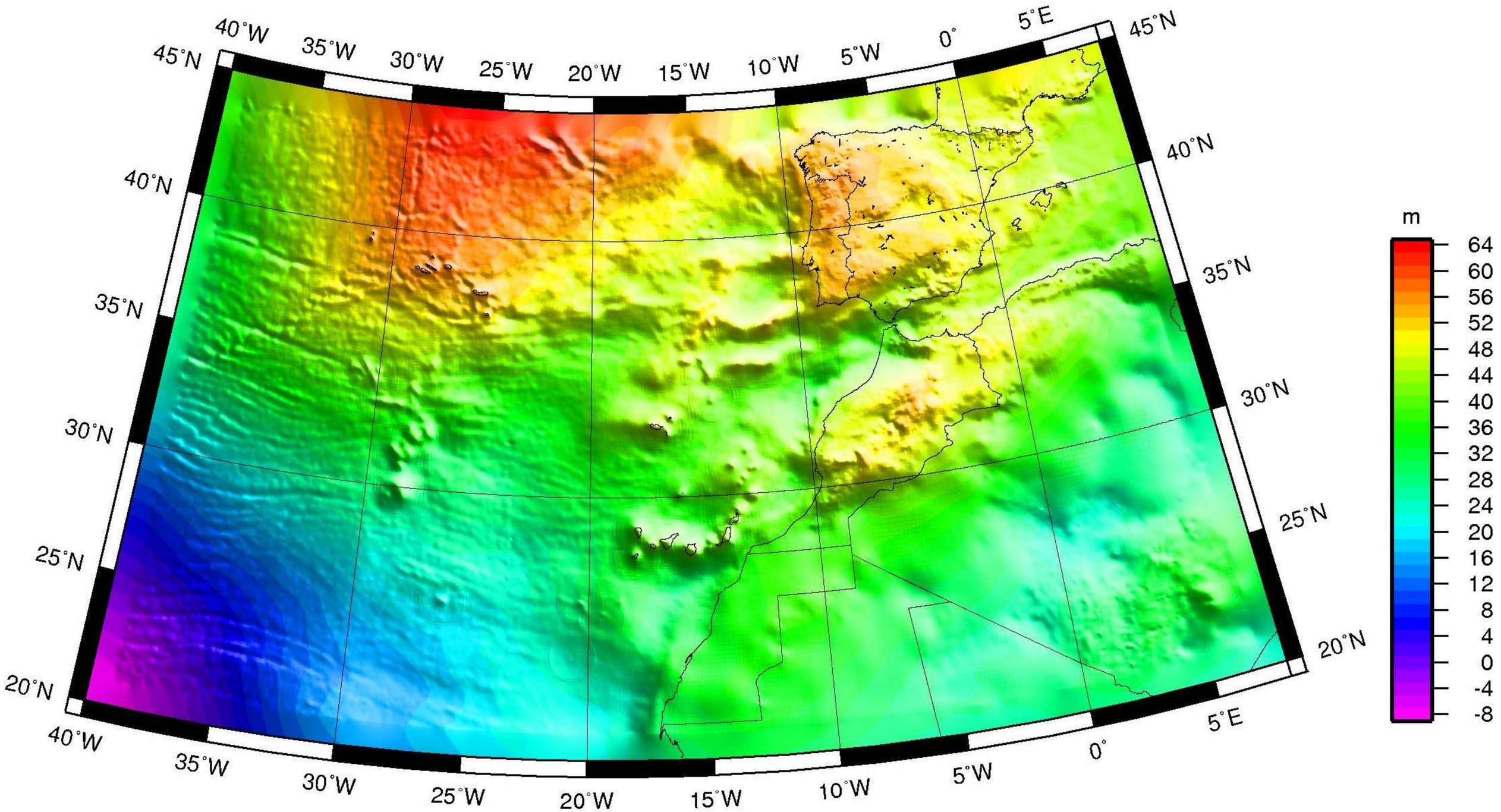
40°W
35°W
30°W
25°W
20°W
15°W
10°W
5°W
0°
5°E
45°N
40°N
35°N
30°N
25°N
20°N
m
64
60
56
52
48
44
40
36
32
28
24
20
16
12
8
4
0
-4
-8

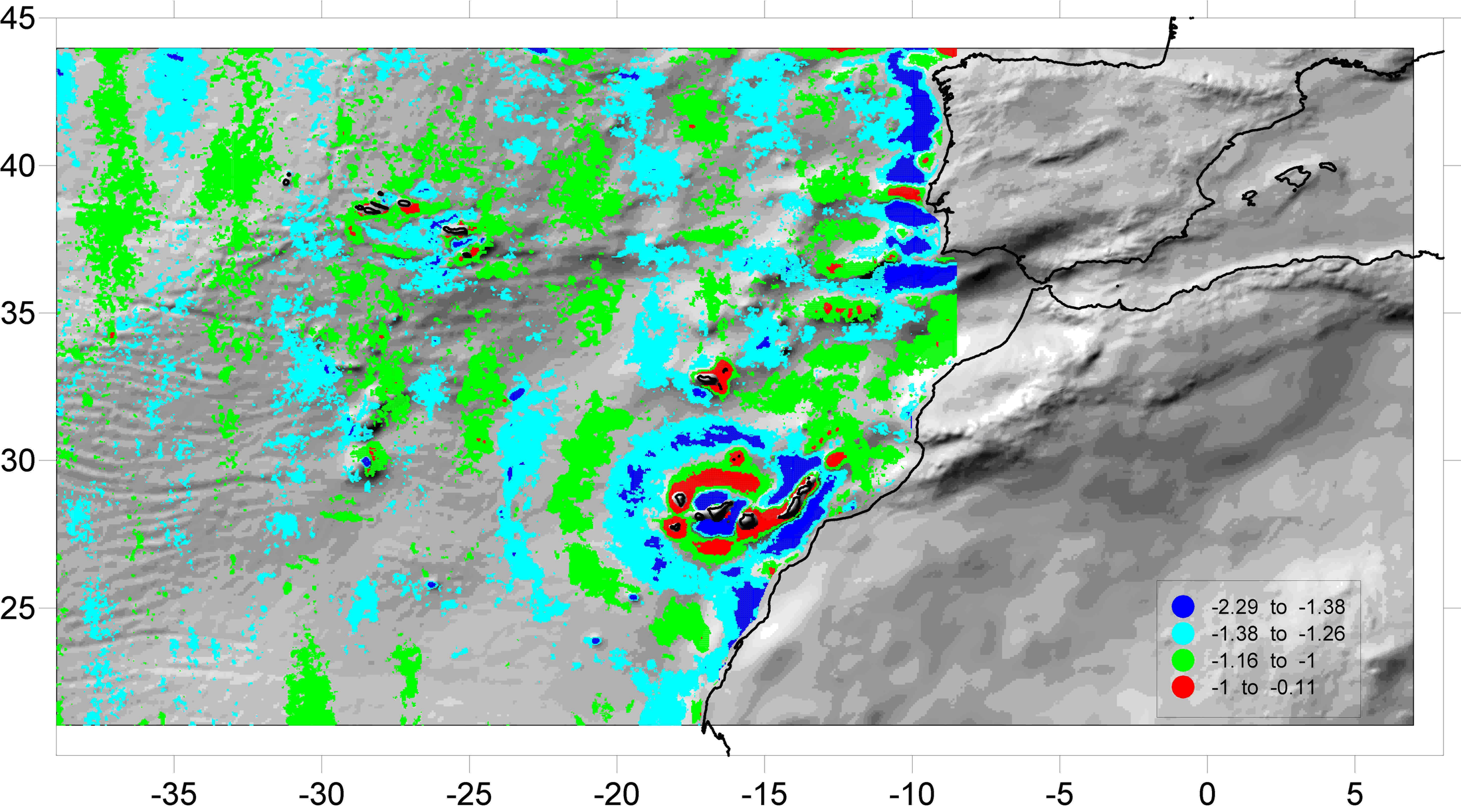
45
40
35
30
25
-35
-30
-25
-20
-15
-10
-5
0
5
-2.29 to -1.38
-1.38 to -1.26
-1.16 to -1
-1 to -0.11